Substrate identification and treatment of right ventricular tachycardia: scar patterns and novel mapping tools

Venlet, J.

CHAPTER 5

5

RV tissue heterogeneity on CT: A Novel Tool to identify the VT Substrate in ARVC

Jeroen Venlet[1], MD; Qian Tao[2*] PhD; Michiel de Graaf[1], MD, PhD; C. Glashan[1], MD1; Marta de Riva Silva[1], MD; Rob Van der Geest[2], PhD; Arthur J. Scholte[1], MD, PhD; Sebastiaan R.D Piers[1], MD, PhD; Katja Zeppenfeld[1], MD, PhD.

1. Department of Cardiology, Leiden University Medical Center, Leiden, the Netherlands
2. Department of LKEB, Leiden University Medical Center, Leiden, the Netherlands
* Contributed equally to the manuscript

JACC Clin Electrophysiol. 2020 Sep;6(9):1073-1085

Abstract

Objectives

This study sought to evaluate whether right ventricular (RV) tissue heterogeneity on computed tomography (CT): 1) is associated with conduction delay in arrhythmogenic right ventricular cardiomyopathy (ARVC); and 2) distinguishes patients with ARVC from those with exercise-induced arrhythmogenic remodeling (EIAR) and control individuals.

Background

ARVC is characterized by fibrofatty replacement, related to conduction delay and ventricular tachycardias. Distinguishing ARVC from acquired, (EIAR) is challenging.

Methods

Patients with ARVC or EIAR and combined endocardial-epicardial electroanatomical voltage mapping for VT ablation with CT integration were enrolled. Patients without structural heart disease served as control individuals. Tissue heterogeneity on CT (CT heterogeneity) was automatically quantified within the 2-mm subepicardium of the entire RV free wall at normal sites and low voltage sites harboring late potentials (LP+) in ARVC/EIAR.

Results

Seventeen patients with ARVC (15 males; age: 50 ± 17 years), 9 patients with EIAR (7 males; age: 45 ± 14 years) and 17 control individuals (14 males; age: 50 ± 15 years) were enrolled. Of 5215 ARVC mapping points, 560 (11%) showed LP+. CT heterogeneity was higher at sites with LP+ compared to normal sites (median: 31 HU/mm; IQR: 23 to 46 HU/mm vs. median: 16 HU/mm; IQR: 13 to 21 HU/mm; $p < 0.001$). The optimal CT heterogeneity cutoff for detection of LP+ was 25 HU/mm (area under the curve [AUC]: 0.80; sensitivity: 72%; specificity: 78%). Overall CT heterogeneity allowed highly accurate differentiation between patients with ARVC and control individuals (AUC: 0.97; sensitivity: 100%; specificity: 82%) and between ARVC and EIAR (AUC: 0.78; sensitivity: 65%; specificity: 89%).

Conclusions

In patients with ARVC, tissue heterogeneity on CT can be used to identify LP+ as a surrogate for ventricular tachycardia substrate. The overall tissue heterogeneity on CT allows the distinguishing of patients with ARVC from those with EIAR and control individuals.

Introduction

Arrhythmogenic right ventricular (RV) cardiomyopathy (ARVC) is a hereditary disease characterized by fibrofatty replacement of myocardium, progressing from the epicardium towards the endocardium.[1-3] Heterogeneous tissue provides the substrate for slow conduction facilitating re-entrant ventricular tachycardia (VT).[4] Isolated late potentials (LPs) within low voltage regions reflect delayed activation of excitable tissue or sites protected by areas of fixed or functional block and are considered a surrogate for VT substrate.[5, 6]

Cardiac computed tomography (CT) allows delineation of fat and myocardium with high spatial resolution.[7-9] The percentage of intramyocardial fat within the RV, quantified on CT, has been demonstrated to be higher in patients with ARVC compared to matched controls [7] and local abnormal ventricular electrograms have been related to areas with a high percentage of intramyocardial fat.[10] However, high percentages of fat may be also due to confluent areas of intramyocardial fat, which result in local abnormal low voltage electrograms not related to VT.

An important differential diagnosis with clinical and prognostic implications is exercise-induced arrhythmogenic remodeling (EIAR), which can mimic early ARVC.[11] EIAR is characterized by an isolated subepicardial RV outflow tract (RVOT) scar serving as substrate for fast VT in high-level endurance athletes.[11] The specific histopathology is unknown, and distinguishing this acquired entity from inherited ARVC can be challenging.[11]

In the present study we propose a novel CT-derived parameter reflecting local tissue heterogeneity, further referred to as CT heterogeneity. We hypothesize that (1) increased CT heterogeneity is associated with conduction delay, allowing for non-invasive identification of the VT substrate in ARVC; and (2) the overall CT heterogeneity may distinguish ARVC from EIAR and control individuals.

Methods

Patients

Consecutive patients with VT due to ARVC or EIAR who underwent detailed combined endocardial-epicardial RV electroanatomical mapping (EAM) during sinus rhythm and VT ablation with real-time integration of CT between 2006 and 2015 were enrolled. Two patients with incomplete RV EAM were excluded from analysis. The diagnosis of

ARVC was established using the 2010 revised Task Force Criteria.[12] Mutations were classified as previously described.[13] The diagnosis of EIAR was based on the presence of VT related to an isolated RVOT scar in endurance athlete, after exclusion of ARVC and sarcoidosis.[11]

The control group consisted of patients without a history of ventricular arrhythmias, abnormal findings on electrocardiography (ECG), or structural heart disease who underwent cardiac CT for exclusion of significant coronary artery disease.

The study was approved by the local ethical committee. All patients provided informed consent before the mapping and ablation procedure.

Computed tomography acquisition and preprocessing

ECG-gated CT imaging were performed with either a 64-detector row (Aquilion 64, Toshiba Medical Systems, Otawara Japan) or a 320-detector row CT scanner (Aquilion ONE, Toshiba Medical Systems) with an intravenous iodinated contrast agent. Images were acquired after an bolus of 69 ± 13 mL of contrast. CT scans were performed with a standard protocol to visualize the coronary arteries. Post-processing of scans was performed with application of dedicated software (Mass, V2013-EXP LKEB, Leiden, the Netherlands). Contours were manually traced on short-axis CT slices (2 mm thickness, 2-mm interslice gap) around the epicardium and pericardium, left ventricle endocardium and aorta. Radiation dose was estimated with a dose-length product conversion factor of 0.014 mSv/(mGy x cm).[14] The original CT data and the 3D contours were imported into the EAM system before mapping and ablation (Figure 1).[15, 16]

Electroanatomical mapping

All antiarrhythmic drugs were discontinued for ≥5 half-lives if possible, with the exception of amiodarone. Epicardial access was obtained through subxiphoid puncture. EAM of the RV endocardium and epicardium was performed during sinus rhythm or RV-pacing (if pacing dependent, n=3) using a 3.5-mm irrigated-tip catheter (NaviStar Thermocool, Biosense Webster Inc, Diamond Bar, California) and the CARTO system. Electrograms were filtered at 30-400 Hz (bipolar) and 1-240 Hz (unipolar). The CT-derived images and EAM were aligned using the left main as a landmark as previously described.[15, 16] Electroanatomical data obtained during remapping after radiofrequency delivery were excluded from the analysis.

Figure 1. Processing and integration of CT images

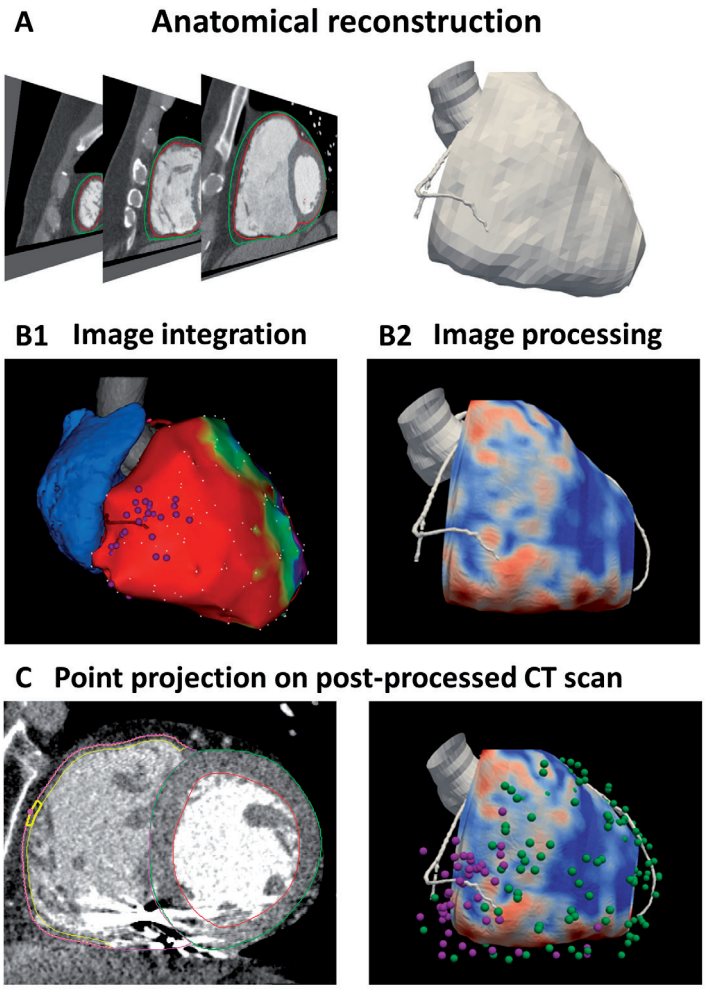

(A) Epicardial **(red)** and pericardial contours **(green)** were traced and, together with coronary anatomy and the original CT data, imported in the CARTO mapping system. **(B, left)** The imported CT images were merged with electroanatomic maps during mapping and ablation. After the procedure, all points were analyzed for the presence of LPs. **(B, right)** CT images were post-processed to quantify tissue heterogeneity. **(C, left)** An example of a mapping point with the corresponding cylinder **(yellow)** projected onto the original CT image. The inferior part of the RV free wall was excluded because of RV lead artifacts. **(C, right)** For post-procedural analysis, electroanatomic mapping points with LP+ **(purple tags)** and without LP **(green)** were projected onto the post-processed CT contours, color coded for the CT heterogeneity. CT = computed tomography; LP = late potential; RV = right ventricle.

Electrogram analysis

All bipolar electrograms were displayed at the same gain (scale bar at 0.14 mV/1cm) and sweep speed (200 mm/s). Bipolar voltage >1.50 mV was considered normal at the endocardium and epicardium. Unipolar voltage >3.90 mV was considered normal at the

endocardium.[17] Late potentials (LP) were defined as inscribing after QRS, separated by isoelectric segment >20 ms.

All mapping points were categorized as:

(A) no scar, defined by normal bipolar and, for endocardial mapping points, normal unipolar voltage (normal point: NP)
(B) scar without LP, defined by abnormal bipolar and/or unipolar voltage but no LP (LP-), or
(C) scar with LP, defined by abnormal bipolar and/or unipolar voltage and the presence of LP (LP+).

Post-procedural analysis

After the procedure, electroanatomical maps and 3D CT contours were exported from the mapping system. Using MATLAB software version R2015b (MathWorks, Natick, Massachusetts), the CT contours and mapping points were projected on the original CT data (resolution 0.36 x 0.36 x 0.36 mm) (Figure 1). Areas with implantable cardioverter defibrillator lead artefact on the CT and the septum were excluded from analysis. Mapping points were excluded if they were projected >10 mm from the contours to exclude points within the cavity or points taking during deep inspiration. In addition, mapping points without LP were excluded if located within close vicinity (<10 mm) of a site with LP+.

CT-derived tissue heterogeneity and intramyocardial fat

Tissue heterogeneity on CT was analyzed in the inner 2 mm rim from the RV free wall epicardial contour because of the known disease progression from the epicardium towards the endocadium in ARVC.[3] First, to analyze CT-derived tissue heterogeneity at each mapping site, a region of interest was defined as a cylinder-shaped region (height: 2 mm; radius: 5 mm; volume $\prod . r2 . h$, 157 mm^3), centered at the catheter tip projection, on the RV free wall. The computation of tissue heterogeneity consisted of two steps: (1) the image gradient within the region of interest was first computed over the full range of Hounsfield units (HU), reflecting local tissue change, i.e. the potential transition between fibrofatty tissue and normal myocardium, (2) the SD of the gradient was then computed within the region of interest, describing the variation in tissue transition in the sampled tissue. The CT-derived tissue heterogeneity quantified by the SD of the gradient is further referred to as CT heterogeneity (see the Supplemental Methods for the full methodology and Supplemental Figure 1).

In addition, intramyocardial fat was quantified as the percentage of image pixels with ≤ -30 HU within the cylinder.[18, 19]

Both CT heterogeneity and the intramyocardial fat percentage were compared between sites with the predefined 3 categories of mapping points: (A) no scar (NP), (B) scar without LP (LP-), and (C) scar with LP (LP+).

Overall CT-derived tissue heterogeneity and intramyocardial fat per patient

To calculate the overall CT heterogeneity and intramyocardial fat per patient, dense, uniform sampling of the entire RV free wall was performed with the sampling cylinders (radius: 5 mm; height: 2 mm) for each patient (central illustration). The overall CT heterogeneity and intramyocardial fat percentage were compared between patients with ARVC, those with EIAR, and control individuals.

Statistical analysis

Categorical variables are displayed as number (percentage) and continuous variables are expressed as mean ± SD or median (interquartile range). Continuous variables were compared using the Unpaired t-test, Mann-Whitney U Test, Kruskal-Wallis for the omnibus test, the Dunn-Bonferroni for the pairwise comparisons with the Bonferroni Correction. Categorical variables were compared by using the chi-square test. Receiver operating characteristics curve analysis was performed to determine the optimal cutoff value, defined as the value maximizing the sum of sensitivity and specificity. All tests were 2-sided and P-values <0.05 were considered statistically significant. All analyses were performed with SPSS version 23.0 (IBM SPSS, Armonk, NY).

Results

Patients

A total of 17 patients with ARVC (age 50 ± 17 years, 15 [88%] male, body mass index [BMI] 25 ± 4 kg/m^2) and 9 patients with EIAR (age 45 ± 14 years, 7 [78%] male, BMI 23 ± 3 kg/m2), who underwent combined endocardial-epicardial EAM and CT image integration were enrolled (baseline characteristics are provided in Table 1). The control group consisted of 17 patients (age 50 ± 15 years, 14 [82%] male, BMI 25 ± 5 kg/m^2). There were no significant differences in age, sex, BMI and history of diabetes mellitus or hypertension between patients with ARVC, patients with EIAR and individuals control. Mean radiation dose for the CT scan was 3.3 ± 1.8 mSv.

Table 1. Baseline characteristics

	ARVC (n=17)	EIAR (n=9)
Age, years	50±17	45±14
Sex (male)	15 (88%)	7 (78%)
BMI (kg/m^2)	25±4	23±3
Diabetes	1 (6%)	0 (0%)
Hypertension	2 (12%)	1 (11%)
First presentation		
OHCA	3 (18%)	0 (0%)
(pre) syncope	1 (6%)	5 (56%)
Palpitations	11 (65%)	3 (33%)
Other	2 (12%)	1 (11%)
ECG		
Epsilon wave	5 (29%)	0 (0%)
TAD >55 ms	10/13	0/8
TWI V1-V3	8 (47%)	0 (0%)
TWI V1- V2	1 (6%)	2 (22%)
TWI V1-V4 (RBBB)	3 (18%)	0 (0%)
TWI V4-V6	4 (24%)	0 (0%)
TWI inferior	3 (18%)	0 (0%)
Imaging		
CMR	9	7
WMA or aneurysm	5/9 (56%)	0/7 (0%)
RVEDV ml/m^2	119±29	136±19
RVEF	44±8	46±3
LVEDV ml/m^2	89±18	113±17
LVEF	56±6	55±4
Echocardiography	8*	2*
WMA or aneurysm	6/8 (75%)	0
PLAX RVOT index mm/ m^2	23±3	22±6
PSAX RVOT index mm/ m^2	22±3	22±6
RV FAC, %	27±11	33±11
Family history	5 (29%)	0 (0%)
Pathogenic mutation		
Desmosomal	11 (65%)	0 (0%)
ARVC associated	13 (77%)	0 (0%)

Variables are expressed as mean ± SD or n/N (%). ARVC denotes arrhythmogenic right ventricular cardiomyopathy; BMI, body mass index; CMR, cardiac magnetic resonance; EIAR, exercise induced arrhythmogenic remodeling; FAC, fractional area change; LVEDV, left ventricular end diastolic volume, LVEF, LV ejection fraction; OHCA, out of hospital cardiac arrest; RBBB, right bundle branch block; RVEDV, right ventricular end diastolic volume; RVEF, RV ejection fraction; TAD, terminal activation duration; TWI, T-wave inversion; WMA, wall motion abnormalities. * Echocardiography in patients with contraindications for cardiac magnetic resonance imaging.

Electroanatomical mapping

Combined endocardial and epicardial mapping with successful CT image integration was performed in all ARVC and EIAR patients. The average number of mappings points was 221 ± 84 at the RV endocardium and 298 ± 126 at the epicardium.

CT heterogeneity, intramyocardial fat and late potentials

All mapping points were projected on the post-processed CT scan. After exclusion of all points located >10 mm from the CT contours and all points without LP but located <10 mm from points with LP+, a total of 7777 points remained and were selected for analysis, including 5215 points in ARVC patients and 2562 points in patients with EIAR. Of the 5215 mapping points in ARVC, 560 (11%) points demonstrated scar with LP (LP+). The CT heterogeneity at mapping points in ARVC patients had a median value of 19 HU/mm (IQR 15-26 HU/mm). CT heterogeneity was significantly higher at LP+ sites compared to normal points (NP) and scar points without LP (LP-) for both the endocardium and epicardium (P<0.001, Table 2, Figures 2 and 3A). NP demonstrated the lowest CT heterogeneity. The optimal CT heterogeneity cutoff value to differentiate between LP+ sites and all other points was 25 HU/mm (area under the curve [AUC]: 0.80; sensitivity: 72%; specificity: 78%, Figure 3C).

Table 2. CT heterogeneity at mapping points in ARVC

	No scar (NP)	Scar no LP (LP-)	Scar and LP (LP+)	P-value
ARVC (n=5215)	16 (13-21)	19 (15-25)	31 (23-46)	<0.001
Endocardium (n=2424)	16 (13-20)	20 (15-29)	30 (25-43)	<0.001
Epicardium (n=2791)	17 (14-22)	18 (15-24)	33 (22-52)	<0.001
EIAR (n=2562)	14 (12-16)	13 (12-16)	13 (12-18)	0.304
Endocardium (n=1139)	13 (12-15)	14 (11-19)	-	0.152
Epicardium (n=1423)	14 (12-16)	13 (12-16)	13 (12-18)	<0.001*

Values are median (interquartile range). LP denotes late potential; NP, normal point. Other abbreviations as in Table 1.

* denotes a statistical difference between NP and LP- but not between the categories LP+ and NP or LP+ and LP-.

Figure 2. Electroanatomical voltage maps and CT heterogeneity

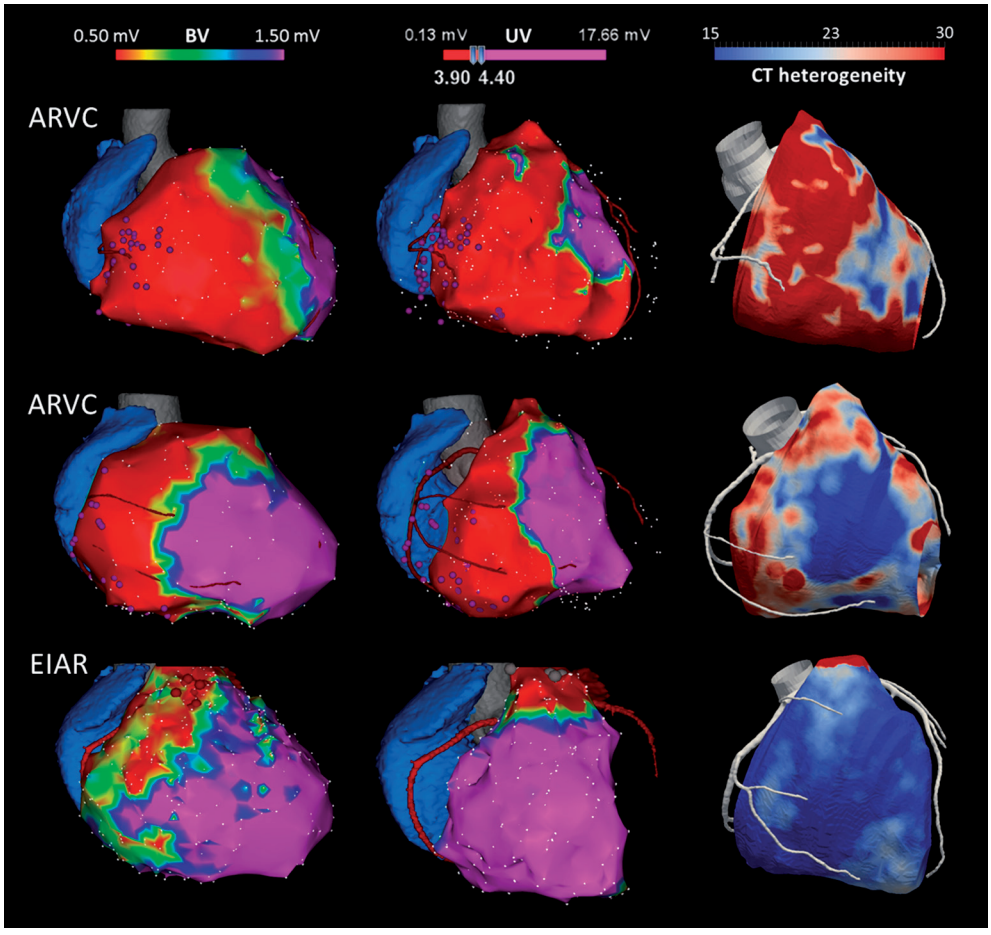

Examples of 2 patients with ARVC and 1 patient with EIAR, with an epicardial bipolar voltage map (BV) on the left; endocardial unipolar voltage map (UV) in the middle; and CT contour, color coded for tissue heterogeneity, on the right. The **purple tags** indicate mapping points with late potentials.

The median percentage of intramyocardial fat in ARVC patients was 12% (IQR 3-29%, Figure 3B). The median percentage of intramyocardial fat was higher at LP+ points compared to NP and LP-. The optimal intramyocardial fat percentage cutoff value for detection of LP sites versus all other points was 6% (AUC: 0.58; sensitivity: 80%; and specificity 37%, Figure 3C).

Figure 3. CT heterogeneity and intramyocardial fat in ARVC

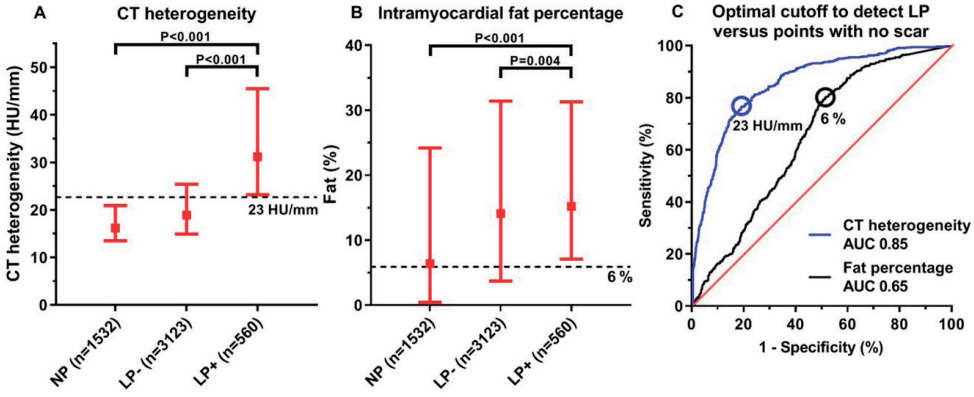

(A, B) The median and interquartile range for CT heterogeneity and intramyocardial fat percentage according to mapping point categories. **(C)** ROC curve for the optimal cutoff to differentiate between scar with LPs (LP+) and all other points. AUC = area under the curve; LP– = scar without LPs; NP = normal point; ROC, receiver operating characteristic; other abbreviations as in Figure 1 and 2.

In EIAR, 74 (3%) of the 2562 mapping points fulfilled the definition of LP+. All LP+ points were located at the epicardium. The CT heterogeneity had a median value of 13 HU/mm (IQR: 12 to 16 HU/mm) and was similar across all three mapping point categories (P=0.304, Table 2, Figure 4A). The median intramyocardial fat percentage was 8% (IQR 0-26%) and higher at sites with LP+ compared to NP (P<0.001), but there was no difference at LP+ versus LP– sites (p >0.999, Figure 4B). Similar to the findings in ARVC, the intramyocardial fat percentage did not allow accurate differentiation between LP+ versus all other points (AUC: 0.59).

Figure 4. CT heterogeneity and fat compared between ARVC and EIAR

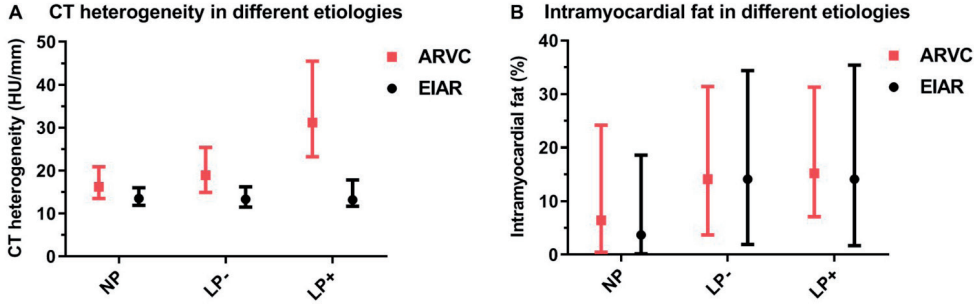

The median and interquartile range for **(A)** CT heterogeneity and **(B)** fat percentage for the point categories for ARVC and EIAR. ARVC showed a significantly higher CT heterogeneity compared to EIAR for all categories, and, in particular, at mapping points with LPs (p < 0.001). The intramyocardial fat percentage did not differ between mapping point categories in ARVC versus LP+ sites in EIAR (all p > 0.05, **B**). NP = no scar; LP– = scar without LP; LP+ = scar with LP. Abbreviations as in Figures 1,2 and 3.

When comparing the patients with ARVC and EIAR, the CT heterogeneity in patients with EIAR was lower compared to patients with ARVC for each of the three mapping point categories (P<0.001, Figure 4A). The intramyocardial fat percentage did not differ between mapping point categories in ARVC vs. LP+ sites in EIAR (all P>0.05, Figure 4B).

Overall CT heterogeneity per patient to differentiate between patients with ARVC, patients with EIAR and control individuals

To compare patients with ARVC, those with EIAR and control individuals, the CT heterogeneity at a mean of 4995 ± 13 uniformly selected sample sites per patient was determined. In patients with ARVC, the median CT heterogeneity was 23 HU/mm (IQR 17-29 HU/mm; mean: 25 ± 9 HU/mm; range 15 to 48 HU/mm), compared to 18 HU/mm (IQR: 14 to 19 HU/mm; mean: 12 ± 2 HU/mm; range 13 to 22 HU/mm) in patients with EIAR and 13 HU/mm (IQR: 11 to 14 HU/mm; mean: 17 ± 3 HU/mm; range 10 to 18 HU/mm) in control individuals (Figure 5, Central Illustration. The optimal CT heterogeneity cutoff value to differentiate between ARVC and control individuals was 15 HU/mm (AUC 0.97, sensitivity 100%, specificity 82%). Of interest, 6 of 17 patients with the final diagnosis ARVC in our cohort did not fulfill any of the Task Force imaging criteria for ARVC. These 6 patients, with an early form of ARVC, could all be correctly identified by using CT heterogeneity.

The median intramyocardial fat percentage in ARVC was 17% (IQR 13-22%) compared to 5% (IQR 3-8%) in control individuals (P<0.001). The intramyocardial fat percentage had a lower accuracy to differentiate between ARVC and controls when compared to CT heterogeneity (AUC 0.90, optimal cutoff value 9%, sensitivity 88%, specificity 88%). In patients with EIAR, the median fat percentage was 18% (IQR 3 to 19%). The intramyocardial fat percentage had no discriminatory capacity to distinguish between ARVC and EIAR (AUC: 0.50).

Figure 5. CT derived heterogeneity images from patients with ARVC, patients with EIAR and control individuals

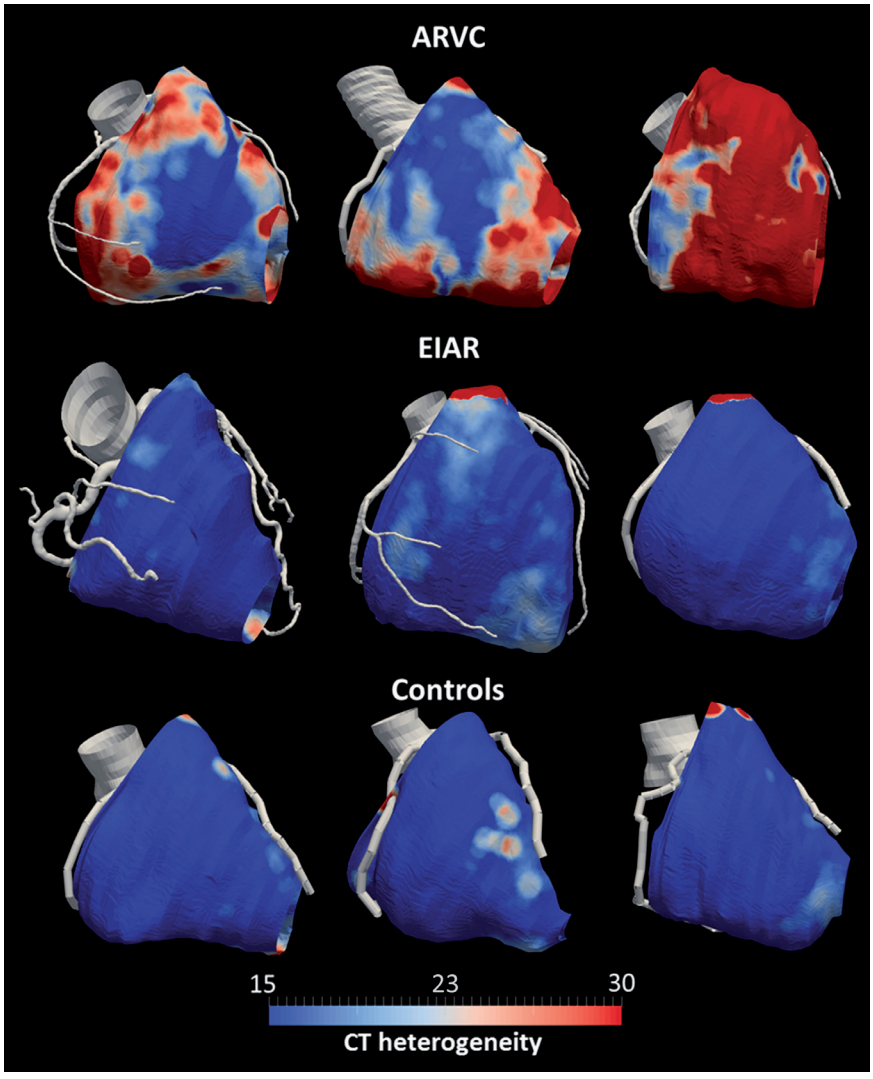

CT-derived heterogeneity in **(A)** patients with ARVC, **(B)** patients with EIAR, and **(C)** healthy control individuals. The tissue heterogeneity in patients with EIAR and control individuals is low (below the optimal CT heterogeneity cutoff of 15 to differentiate between patients with ARVC and control individuals, visualized as **dark blue**, compared to areas with a higher tissue heterogeneity in ARVC. Abbreviations as in Figure 1,2 and 3.

Central illustration

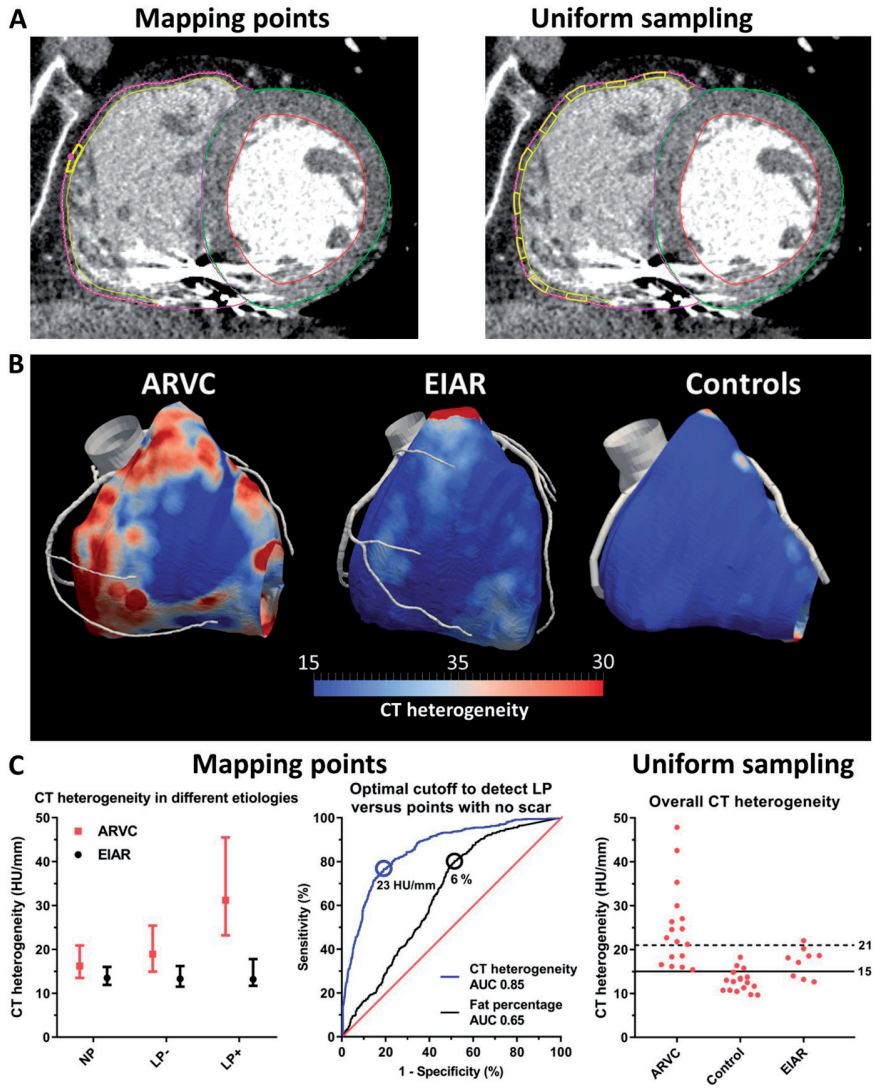

(A) Tissue heterogeneity on CT was analyzed using 5-mm-diameter cylinders in the inner 2-mm rim from the RV free wall epicardial contour, which were applied both for electroanatomic mapping points **(left panel)** and uniformly sampled sites **(right panel)**. **(B)** Examples of CT-derived heterogeneity for a patient with arrhythmogenic RV cardiomyopathy (ARVC), a patient with exercise-induced arrhythmogenic remodeling (EIAR), and a healthy control individual. **(C)** The median and interquartile range for CT heterogeneity for the mapping point categories in ARVC and EIAR **(left panel)** and a comparison of receiver operating characteristic curves **(middle panel)** are shown, demonstrating that CT heterogeneity allowed detection of LP+ with a higher accuracy compared to the intramyocardial fat percentage. The scatter plot **(right panel)** illustrates that the overall CT heterogeneity was higher in patients with ARVC compared to control individuals and patients with EIAR. The optimal cutoff between patients with ARVC and control individuals is depicted by the **black line**, and the optimal cutoff between ARVC and EIAR by the **dashed line**. ARVC = arrhythmogenic right ventricular cardiomyopathy; CT = computed tomography; EIAR = exercise induced arrhythmogenic remodeling; HU = Hounsfield unit; RV = right ventricle.

Discussion

The present study is the first to analyze tissue heterogeneity on CT as a novel tool for identification of an arrhythmogenic substrate in patients with ARVC, and to distinguish ARVC from EIAR and control individuals.

The findings can be summarized as follows: 1) the newly proposed measure of tissue heterogeneity derived from CT allowed the detection of electroanatomic sites with LP+ as a surrogate for VT substrate in patients with ARVC, but not in those with EIAR, suggesting a disease-specific diagnostic tool; and 2) the overall CT heterogeneity allowed highly accurate differentiation between patients with ARVC, patients with EIAR, and control individuals.

The role of CT in ARVC: physiological or pathophysiological intramyocardial fat?

As a result of the excellent spatial resolution of CT, the presence of intramyocardial fat infiltration on CT has been described in ARVC for more than 2 decades in multiple studies.[8, 9, 20] Despite promising results, CT has not been incorporated in the 2010 ARVC task force criteria,[12] partially due to concerns regarding the differentiation between pathophysiologic and physiologic fatty infiltration and the exposure to radiation.[21] In a recent study, the percentage of RV intramyocardial fat on CT has been proposed as a quantitative parameter to differentiate between patients with ARVC and control individuals.[7]

Of note, substantial amounts of intramyocardial fat have been observed at autopsy in patients with various cardiac diseases and in patients without cardiac disease who died from noncardiac causes.[22, 23] In addition, homogeneous areas of intramyocardial fat or scar attenuate local voltages but may not necessarily be arrhythmogenic. In contrast, heterogeneous tissue may result in slow conduction and functional conduction block, thereby facilitating re-entrant VT. In the present study, it was hypothesized that tissue heterogeneity on CT is associated with conduction delay in ARVC and allows differentiation between patients with ARVC, those with EIAR, and control individuals.

CT heterogeneity: a novel parameter to quantify RV tissue heterogeneity

In this study we propose a novel measure for CT heterogeneity, which may reflect the complexity of fibrofatty infiltration of myocardial tissue, which may be particularly prevalent in ARVC patients. If there is intermingling of fibrofatty tissue and normal myocardium, the tissue transition would be identified by the gradient; if the transition

pattern is complex, the distribution of the gradient values would be more dispersed than if the pattern is simple, leading to a high standard deviation of the gradient value.

From a mathematical point of view, the standard deviation is a second-order statistic, which already describes heterogeneity to a certain extent. However, the standard deviation of HU on the original CT image is insufficient for our purpose of quantifying fibrofatty infiltration, since it is not able to characterize how fibrofatty tissue intermingles with myocardium tissue in a local manner. The local transitions, on the other hand, can be well represented by the gradient. This rationale underlies the proposed metric, the standard deviation of gradient, referred to as CT heterogeneity. Because of: 1) the known disease progression wave front from epicardium to endocardium in ARVC and 2) wall thinning in ARVC, CT heterogeneity was assessed in the 2 mm subepicardial layer. [3, 24]

CT heterogeneity and late potentials in ARVC

LPs within low voltage regions indicate the presence of significant activation delay caused by areas of fixed or functional block, and are considered as surrogates for VT related sites.[5, 6] When CT heterogeneity was compared between the three categories of mapping points, it was highest at sites with LP+, followed by low-voltage sites without evident conduction delay and normal-voltage sites. Of importance, CT heterogeneity was able to differentiate between endocardial and epicardial sites with and without conduction delay, specifically in ARVC patients, with good accuracy (AUC: 0.80; sensitivity: 72%; specificity: 78%, Figure 3C).

One prior study has analyzed electrograms at sites with intramyocardial fat in 16 ARVC patients using integration of CT-derived intramyocardial fat during electroanatomical mapping and found that 80% of electrograms with any local abnormal ventricular activity (LAVA) were located within intramyocardial fat on CT.[10] In the present study, local CT heterogeneity allowed more accurate identification of low voltage sites harboring LP+ as a more specific surrogate for a potential VT substrate than the local percentage of intramyocardial fat (AUC 0.85 for CT heterogeneity vs. 0.65 for intramyocardial fat percentage). This finding supports our hypothesis that tissue heterogeneity on CT may represent a more reliable marker for the arrhythmogenic substrate in ARVC than the percentage of intramyocardial fat.

CT heterogeneity in EIAR

In patients with EIAR, a novel clinical entity of VT related to RVOT scars in extreme endurance athletes,[11] CT-derived tissue heterogeneity did not allow differentiation between sites with and without LP+. Although the potential difference of the anatomical substrate can only be validated by histology, the findings suggest that the newly

proposed measure of CT heterogeneity may detect LP+ only in areas with fibrofatty replacement and support the premise that EIAR and ARVC must be viewed as separate disease entities.[11]

Overall CT heterogeneity: a powerful tool to differentiate between ARVC, EIAR and controls

In the present study, the overall CT heterogeneity allowed highly accurate differentiation between ARVC and controls (AUC 0.97, sensitivity 100%, specificity 82%). A prior study using the percentage of intramyocardial fat reported a similar accuracy to diagnose ARVC. [7] However, when calculated in the current study, the intramyocardial fat percentage was less accurate, with a lower sensitivity (AUC 0.90, sensitivity 88%, specificity 88%). The differences may be partly explained by the applied CT protocols. For the CT acquisition in our study a bolus with a median of 69 ml of contrast was used versus 100 and 120 ml, respectively, in the 2 prior studies with a double contrast protocol. [7, 10] Of importance, less than half of the radiation dosage was required compared to the prior study,[7] which further supports the clinical relevance of the newly proposed measure CT heterogeneity allowing accurate diagnosis with low radiation exposure and small contrast dosages.

As discussed above, the presence of intramyocardial fat may neither be sensitive nor specific for ARVC. In an autopsy study of explanted human hearts, RV intramyocardial fat percentage of >22% had a sensitivity of only 50% to diagnose ARVC.[22] In contrast, substantial amounts of intramyocardial fat have been described in patients without RV cardiomyopathy, both on CT and in autopsy studies.[24-26] The high accuracy of CT heterogeneity for ARVC, which showed a better performance than fat percentage in the present study, suggests that tissue heterogeneity may be a more specific feature of pathological fatty infiltration (Figure 6). However, studies comparing tissue histology and CT heterogeneity are required to validate the present findings.

Of interest, the entire RV free wall was uniformly sampled for overall CT heterogeneity. Whether focusing on ARVC predilection areas, such as the subtricuspid region and RVOT,[27] may further improve the accuracy of the CT heterogeneity for differentiation between ARVC and control individuals needs further studies.

Clinical implications

CT heterogeneity is a novel tool which may be used to identify the arrhythmogenic substrate and guide VT ablation procedures in patients with ARVC. CT is widely available and can easily be obtained in patients with devices. The overall CT heterogeneity allows highly accurate differentiation between ARVC and control individuals. In the current study, only 65% of the patients had a major imaging task force criteria for ARVC,

suggesting that CT heterogeneity may be of significant value for diagnosing early ARVC if it would be incorporated in the TF criteria in the future.

Further research may aim to analyze the value of RV tissue heterogeneity on CT for diagnosing patients with an early stage of ARVC and for risk stratification for ventricular arrhythmias in patients with ARVC. ARVC is a progressive disease and consecutive CT scans may be used for risk stratification in the near future, since radiation dosage below 1 mSv have been reported.

Figure 6. Histology of the RV myocardium in a patient with ARVC

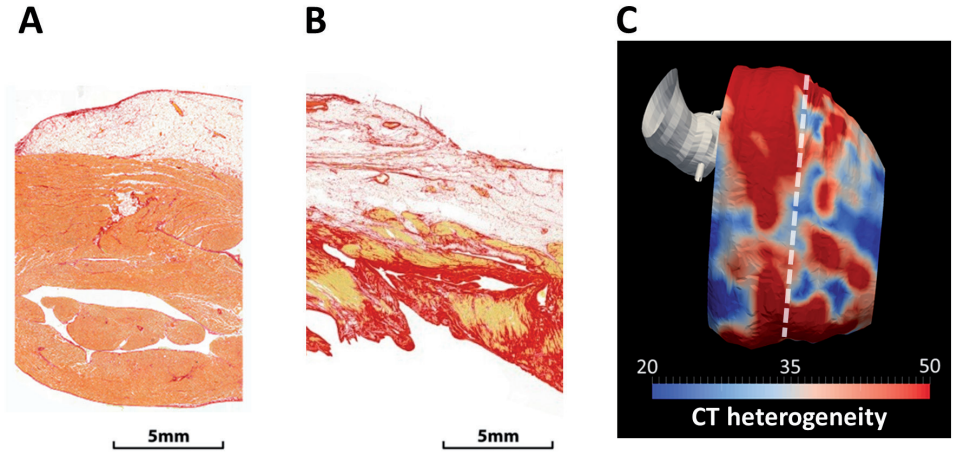

(A) Histology of the RV free wall of a 77-year-old patient without structural heart disease. This slide shows a thick epicardial fat layer **(white)** with minimal fat infiltration between epicardial myocardial fibers. Almost no fibrosis **(red)** is visible in the myocardium. **(B)** Histology of a 72-year-old patient with end-stage ARVC and recurrent ventricular tachycardia (*PKP2*+ mutation), who died of heart failure and acute respiratory distress syndrome. This mid to apical short-axis myocardial slide shows a thick epicardial fat layer covering a very heterogeneous layer of myocardium with a higher percentage of fibrosis fat infiltration between the remaining myocardium. **(C)** A CT-derived heterogeneity image of the same patient with ARVC shows highly heterogeneous tissue in the area of the histological slide. The **dashed line** shows the location of slide. Abbreviations as in Figures 1 and 2.

Limitations

The study was small and only ARVC patients with VT undergoing electroanatomical mapping for VT ablation were enrolled. Therefore, it was impossible to study whether CT heterogeneity can be used for risk stratification for re-entry VT. CT scans were performed to visualize the coronary arteries before an epicardial VT-ablation. The absence of contrast in the RV made it impossible to discern the RV endocardial border in the current study. The CT heterogeneity cutoffs need to be validated in a prospective cohort.

Conclusion

RV tissue heterogeneity, quantified by CT, has a high sensitivity and specificity for detection of low-voltage areas harboring LP+ as potential VT substrate in patients with ARVC. The overall tissue heterogeneity allows for highly accurate differentiation between patients with ARVC, those with EIAR and control individuals. This novel parameter may be an important diagnostic tool to distinguish ARVC from EIAR and normal RV and to guide VT ablation in ARVC patients.

Perspective

Core Clinical Competencies: Tissue heterogeneity on CT can be used to detect areas with late potentials, potentially related to re-entry VT, in patients with ARVC.

Core Clinical Competencies: The overall tissue heterogeneity on CT allowed highly accurate differentiation between ARVC and controls.

Translational Outlook implications: Further studies are needed to evaluate whether tissue heterogeneity may be used to guide VT-ablation in ARVC patients.

Translation Outlook implications 2: Future studies may aim to analyze if tissue heterogeneity on CT can be used as image modality in the ARVC Task Force Criteria and whether it can be used to identify patients with ARVC at risk for re-entry VT.

Reference list

1. Marcus, F.I., et al., *Right ventricular dysplasia: a report of 24 adult cases.* Circulation, 1982. **65**(2): p. 384-98.
2. Thiene, G., et al., *Right ventricular cardiomyopathy and sudden death in young people.* N Engl J Med, 1988. **318**(3): p. 129-33.
3. Basso, C., et al., *Arrhythmogenic right ventricular cardiomyopathy.* Lancet, 2009. **373**(9671): p. 1289-300.
4. Perez-David, E., et al., *Noninvasive identification of ventricular tachycardia-related conducting channels using contrast-enhanced magnetic resonance imaging in patients with chronic myocardial infarction: comparison of signal intensity scar mapping and endocardial voltage mapping.* J Am Coll Cardiol, 2011. **57**(2): p. 184-94.
5. Bogun, F., et al., *Isolated potentials during sinus rhythm and pace-mapping within scars as guides for ablation of post-infarction ventricular tachycardia.* J Am Coll Cardiol, 2006. **47**(10): p. 2013-9.
6. Mountantonakis, S.E., et al., *Relationship between voltage map "channels" and the location of critical isthmus sites in patients with post-infarction cardiomyopathy and ventricular tachycardia.* J Am Coll Cardiol, 2013. **61**(20): p. 2088-95.
7. Cochet, H., et al., *Automated Quantification of Right Ventricular Fat at Contrast-enhanced Cardiac Multidetector CT in Arrhythmogenic Right Ventricular Cardiomyopathy.* Radiology, 2015. **275**(3): p. 683-91.
8. Kimura, F., et al., *Helical CT features of arrhythmogenic right ventricular cardiomyopathy.* Radiographics, 2002. **22**(5): p. 1111-24.
9. Tada, H., et al., *Usefulness of electron-beam computed tomography in arrhythmogenic right ventricular dysplasia. Relationship to electrophysiological abnormalities and left ventricular involvement.* Circulation, 1996. **94**(3): p. 437-44.
10. Komatsu, Y., et al., *Relationship between MDCT-imaged myocardial fat and ventricular tachycardia substrate in arrhythmogenic right ventricular cardiomyopathy.* J Am Heart Assoc, 2014. **3**(4).
11. Venlet, J., et al., *Isolated Subepicardial Right Ventricular Outflow Tract Scar in Athletes With Ventricular Tachycardia.* J Am Coll Cardiol, 2017. **69**(5): p. 497-507.
12. Marcus, F.I., et al., *Diagnosis of arrhythmogenic right ventricular cardiomyopathy/dysplasia: proposed modification of the Task Force Criteria.* Eur Heart J, 2010. **31**(7): p. 806-14.
13. Bhonsale, A., et al., *Impact of genotype on clinical course in arrhythmogenic right ventricular dysplasia/cardiomyopathy-associated mutation carriers.* Eur Heart J, 2015. **36**(14): p. 847-55.
14. Ahmed, W., et al., *Automatic detection and quantification of the Agatston coronary artery calcium score on contrast computed tomography angiography.* Int J Cardiovasc Imaging, 2015. **31**(1): p. 151-61.
15. van Huls van Taxis, C.F., et al., *Real-time integration of MDCT-derived coronary anatomy and epicardial fat: impact on epicardial electroanatomic mapping and ablation for ventricular arrhythmias.* JACC Cardiovasc Imaging, 2013. **6**(1): p. 42-52.
16. Piers, S.R., et al., *Epicardial substrate mapping for ventricular tachycardia ablation in patients with non-ischaemic cardiomyopathy: a new algorithm to differentiate between scar and viable myocardium developed by simultaneous integration of computed tomography and contrast-enhanced magnetic resonance imaging.* Eur Heart J, 2013. **34**(8): p. 586-96.

17. Venlet, J., et al., *Unipolar Endocardial Voltage Mapping in the Right Ventricle: Optimal Cutoff Values Correcting for Computed Tomography-Derived Epicardial Fat Thickness and Their Clinical Value for Substrate Delineation.* Circ Arrhythm Electrophysiol, 2017. **10**(8).
18. Rossner, S., et al., *Adipose tissue determinations in cadavers--a comparison between cross-sectional planimetry and computed tomography.* Int J Obes, 1990. **14**(10): p. 893-902.
19. Yoshizumi, T., et al., *Abdominal fat: standardized technique for measurement at CT.* Radiology, 1999. **211**(1): p. 283-6.
20. Hamada, S., et al., *Arrhythmogenic right ventricular dysplasia: evaluation with electron-beam CT.* Radiology, 1993. **187**(3): p. 723-7.
21. Kimura, F., et al., *Myocardial fat at cardiac imaging: how can we differentiate pathologic from physiologic fatty infiltration?* Radiographics, 2010. **30**(6): p. 1587-602.
22. Basso, C., et al., *Quantitative assessment of endomyocardial biopsy in arrhythmogenic right ventricular cardiomyopathy/dysplasia: an in vitro validation of diagnostic criteria.* Eur Heart J, 2008. **29**(22): p. 2760-71.
23. Cannavale, G., et al., *Fatty Images of the Heart: Spectrum of Normal and Pathological Findings by Computed Tomography and Cardiac Magnetic Resonance Imaging.* Biomed Res Int, 2018. **2018**: p. 5610347.
24. Burke, A.P., et al., *Arrhythmogenic right ventricular cardiomyopathy and fatty replacement of the right ventricular myocardium: are they different diseases?* Circulation, 1998. **97**(16): p. 1571-80.
25. Shirani, J., K. Berezowski, and W.C. Roberts, *Quantitative measurement of normal and excessive (cor adiposum) subepicardial adipose tissue, its clinical significance, and its effect on electrocardiographic QRS voltage.* Am J Cardiol, 1995. **76**(5): p. 414-8.
26. Kim, E., et al., *Right ventricular fat infiltration in asymptomatic subjects: observations from ECG-gated 16-slice multidetector CT.* J Comput Assist Tomogr, 2007. **31**(1): p. 22-8.
27. Te Riele, A.S., et al., *Mutation-positive arrhythmogenic right ventricular dysplasia/cardiomyopathy: the triangle of dysplasia displaced.* J Cardiovasc Electrophysiol, 2013. **24**(12): p. 1311-20.

Supplemental Material

Supplemental Methods

Gradient measures the rate of local change in images or volumes. Gradient is directional; the gradients in the x-, y-, and z-direction of a 3D volume are defined as:

$$g_x = df(x,y,z)/dx$$

$$g_y = df(x,y,z)/dy$$

$$g_z = df(x,y,z)/dz$$

where g_x and g_y are the in-plane horizontal and vertical gradient, and g_z is the through-plane gradient. $f(x,y,z)$ is the acquired CT volume with grid x, y, and z.

g_x is interpreted as the change of Hounsfield Unit per millimetre in the x-direction. In a 3D CT volume, change of Hounsfield Unit occurs in all three directions. The magnitude of the change is calculated as:

$$g = \sqrt{g_x^2 + g_y^2 + g_z^2}$$

The gradient magnitude g describes the rate of Hounsfield change considering all directions.

To quantify the heterogeneity in local tissue, we take the standard deviation (STD) of the gradient value g over the 3D region of interest (ROI), defined as a cylinder-shaped region (height 2 mm, radius 5 mm) as described in the article:

$$SD_g = \sqrt{\frac{\sum_{i=1}^{N}(g - \bar{g})^2}{N}}$$

where N is the number of voxels in the ROI, and $\bar{g}$ is the mean gradient in the ROI.

SD_g quantifies how uniform the gradient is in a defined region. In very homogenous tissue, the standard deviation of gradient is close to zero; in highly heterogeneous tissue, the gradient pattern is complex, and the standard deviation of gradient is high.

The overall gradient was calculated by uniform sampling of the entire RV epicardium using these cylinders.

Supplemental Figures

Supplemental figure 1 provides an intuitive example to compare our heterogeneity measure to the standard deviation measure of image intensity. It shows that the STD gradient constantly increases when the local heterogeneity increases, while the STD intensity does not react to the change as the histogram of the voxels stay similar in all images.

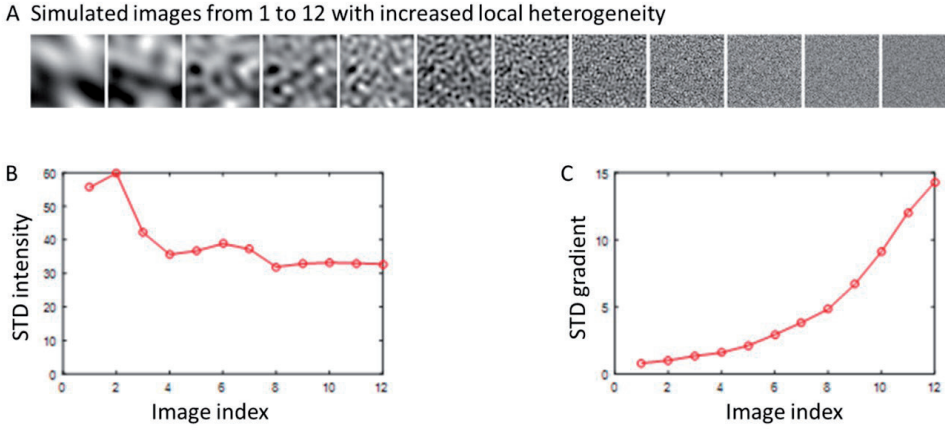

Illustration of the heterogeneity measurement. A. Simulated images with increasing local heterogeneity. B. STD of image intensity on the simulated images. C. STD of the image gradient on the simulated images.